 CMES, vol.50, no.3, pp.253-283, 2009

Molecular Dynamics Analysis of the Instability for a Nano-Scale Liquid Thread

Chun-Lang Yeh[1]

Abstract: This paper investigates the instability of a liquid thread by molecular dynamics (MD) simulation. The influences of liquid thread radius, fundamental cell length, and temperature are discussed. Snapshots of molecules, number of liquid particles formed, and density field are analyzed. Two linear stability criteria, namely Rayleigh's stability criterion and Kim's stability criterion, are accessed for their validity in molecular scale. It is found that a liquid thread is more unstable and produces more liquid particles in the fundamental cell when it is thinner or at a higher temperature. In addition, a liquid thread with a longer fundamental cell length is also more unstable and produces more liquid particles in the fundamental cell, but it evaporates slower. The trends of linear stability theories agree with MD simulation results. However, Rayleigh's stability criterion overpredicts stable domain as compared to the MD simulation results. Kim's stability criterion gives more accurate predictions but overpredicts the stable domain at a higher temperature. Finally, a liquid thread with a higher time averaged density uniformity factor,$\overline{f_\rho}$, is more unstable and produces more liquid particles in the fundamental cell.

Keywords: Nano-Scale Liquid Thread, Molecular Dynamics Simulation, Rayleigh's stability criterion, Kim's stability criterion

Nomenclature

k_B	Boltzmann constant
L	fundamental cell length
m	molecular mass
N	number of molecules
Np	number of liquid particles produced in the fundamental cell

[1] Corresponding Author. Department of Aeronautical Engineering, National Formosa University, Huwei, Yunlin 632, Taiwan, R.O.C., Tel. No.: 886-5-6315527, Fax No.: 886-5-6312415, E-mail: clyeh@nfu.edu.tw

R liquid thread radius
r intermolecular distance
r_c cut-off radius of Lennard-Jones potential function
T temperature
t time
Δt time step
V volume
v_i velocity of molecule i
x, y, z Cartesian coordinates

Greek

ε energy parameter of Lennard-Jones potential function
ρ density
σ length parameter of Lennard-Jones potential function
ϕ Lennard-Jones potential function

Subscripts

L liquid phase
V vapor phase

Superscripts

* non-dimensionalized quantity
_ averaged quantity

1 Introduction

In the scope of fluid flow researches, the instability has received much attention due to its potential influence on the flow development. Previous instability analyses were focused mainly on large scale flow fields. The applicabilities of these theories to micro- or nano-scale flow fields are still uncertain. Lord Rayleigh (1879) studied the instability of cylindrical thin films. He analyzed an inviscid liquid cylinder and a viscous one. Later on, Weber (1931) and Tomotika (1935) considered more realistic cases of liquid threads in unbounded domains.

To establish a nano-scale system is still a complex task because of the major challenges for fabricating the nano-locating and nano-driving assemblies. On the other hand, molecular dynamics (MD) can offer novel insights into the underlying atomistic mechanisms and nano-scale behavior due to their high temporal and spatial resolution. Liu and Tsai (2009)proposed a numerical method for extracting the thermo-mechanical properties of a thin-film. In their study, MD simulations were utilized to establish the load-displacement response of a thin copper substrate. Nair, Farkas, and Kriz (2008)studied the indentation response of Ni thin films of thicknesses in the nano-scale using MD simulations with embedded atom method (EAM) inter-atomic potentials. Their simulation results showed that the contact stress necessary to emit the first dislocation under the indenter is nearly independent of film thickness and that in the elastic regime, the loading curves observed start deviating from the Hertzian predictions for indentation depths greater than 2.5% of the film thickness. Namilae, Chandra, Srinivasan and Chandra (2007)used parallel MD simulations to understand the mechanical behavior of interfaces in carbon nano-tubes (CNTs)based composites. It is shown that interface strength based on non bonded interactions is very low (of the order of few MPa) and it can be significantly improved through surface chemical modification of CNTs (to an order of a few GPa). It is further noted that chemical bonding between functionalized nanotube and matrix during processing is essential to obtain good interface strength and hence a better composite. Tang and Advani (2007)performed non-equilibrium MD simulations to investigate water flow around a single-walled CNT. It was shown that classical continuum mechanics does not hold when the drag forces on the nano-tube are considered. Later, they (2008)proposed a method for studying nanotube dynamics in simple shear flow. In their method, the forces on the nano-tube were obtained by MD simulations. The viscosity of dilute nano-tube suspensions was calculated based on the nano-tube dynamics and the effects of the aspect ratio and initial curvature of the nano-tube on suspension viscosity were explored and discussed. Chen, Cheng and Hsu (2007)evaluated the fundamental mechanical properties of single/multi-walled CNTs using MD simulations. The force field between two carbon atoms is modeled with the Tersoff-Brenner potential while the inlayer/interlayer van der Waals (vdW) atomistic interactions are simulated with the Lennard-Jones potential. They found that the effect of the inlayer vdW atomistic interactions can not be neglected and should receive attention in the MD simulations of the mechanical properties of CNTs. Matsumoto, Nakagaki, Nakatani and Kitagawa (2005)studied the internal structure-changes around the crack tip and the pertinent crack growth behavior in an amorphous metal by MD simulation. The Finnis-Sinclair potential for α-iron was used to describe the inter-atomic potential. Computed results showed that nano-scale crystalline phase grows around the crack tip and that the distribution of deformation zones and deformation mechanism are

significantly altered. Wei, Srivastava and Cho (2002)investigated the temperature dependence of the plastic collapse of single-walled CNTs under axial compression by classical MD simulations using Tersoff-Brenner potential for C-C interactions. The thermal fluctuations are shown to drive nano-tubes to overcome the energy barriers leading to plastically collapsed structures which have significantly lower strain energy than fins-like structure.

In Fig.1, the fluid/air interface for atomizer flow by macroscopic analysis from the author's previous studies [Yeh (2005, 2009)] is shown. It can be seen that the liquid evolves into threads after leaving the atomizer. The formation of liquid threads is one of the most fundamental and important phenomena during the atomization process. Goren (1962) studied the annular liquid films in contact with a solid, i.e., supported on a wire or lining the interior walls of a capillary. He used linear stability analysis to determine the fastest growing mode when either inertia or viscous forces are negligible. Koplik and Banavar (1993) studied the Rayleigh's instability of a cylindrical liquid thread in vacuum by three-dimensional MD simulation. The maximum number of molecules they used consists of 8,192 liquid argon Lennard-Jones molecules for a cylindrical liquid thread of non-dimensionalized radius of 7.5 in a box of non-dimensionalized length of 54.7. For this simulation condition, only one liquid particle was formed. If a smaller computational domain was used instead, no liquid particle was found from their study. Kawano (1998) applied 10,278 Lennard-Jones molecules of liquid and vapor coexisting argon in three dimensions to analyze the interfacial motion of a cylindrical liquid thread of non-dimensionalized radii of 2.0 to 4.0 in a box of non-dimensionalized length up to 120. For this condition of larger computational domain, a maximum number of 8 to 9 liquid particles were observed. Min and Wong (2006) studied the Rayleigh's instability of nanometer scale Lennard-Jones liquid threads by MD simulation and concluded that Rayleigh's continuum prediction holds down to the molecular scale. Kim, Lee, Han and Park (2006) applied MD simulation to investigate the thermodynamic properties and stability characteristics of the nano-scale liquid thread. They found that the overall trends of the simulation results agree with the classical stability theory. However, the classical theory overpredicts the region of stable domain compared to the MD results as the radius decreases.

In the following discussion, the instability of a liquid thread is investigated by MD simulation. The influences of liquid thread radius, fundamental cell length, and temperature will be discussed. Snapshots of molecules, number of liquid particles formed, and density field are analyzed. Two linear stability criteria, namely Rayleigh's stability criterion and Kim's stability criterion, are accessed for their validity in molecular scale. This can provide insights into the mechanism and prediction of the atomization process.

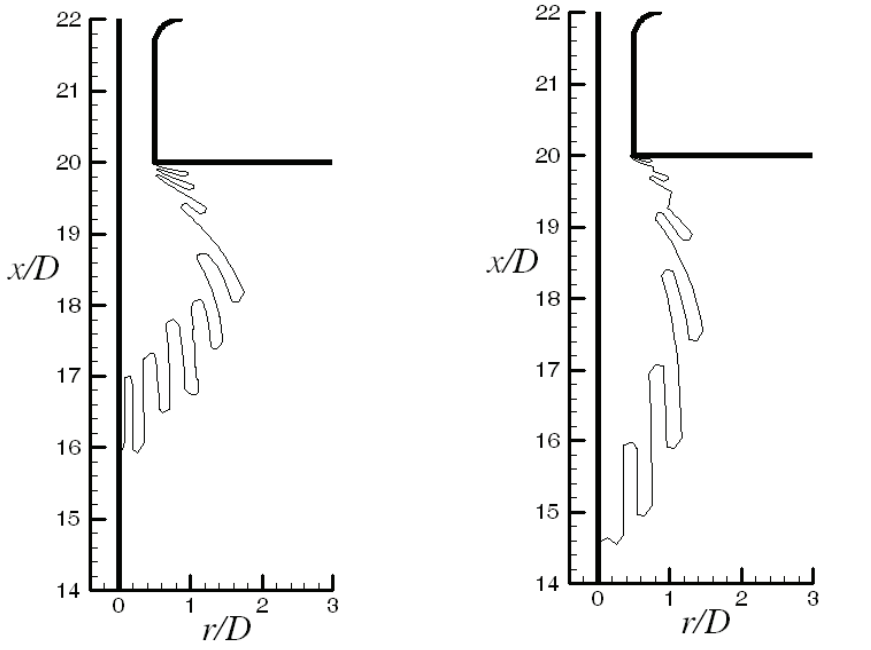

(a) by standard k- ε model (b) by Gatski-Speziale's ARSM model

Figure 1: Fluid/air interface for atomizer flow by macroscopic analysis [Yeh (2005)]

2 Molecular Dynamics Simulation Method

In this study, the vaporization process of a liquid thread is investigated by MD simulation. The inter-atomic potential is one of the most important parts of MD simulation. Many possible potential models exist, such as hard sphere, soft sphere, square well, etc [Haile (1992)]. In this research, the Lennard-Jones 12-6 potential model, which is widely used, is adopted for calculation. It is

$$\phi(r) = 4\varepsilon \left[\left(\frac{\sigma}{r}\right)^{12} - \left(\frac{\sigma}{r}\right)^{6} \right] \tag{1}$$

where r denotes the distance between two molecules, ε and σ are the representative scales of energy and length, respectively. The Lennard-Jones fluid in this research

is taken to be argon for its ease of physical understanding. The parameters for argon are as follows [Kawano (1998)] : the length parameter σ=0.354 nm, the energy parameter ε/k_B=93.3K, and the molecular weight m=6.64$\times 10^{-26}$ kg, where k_B=1.38$\times 10^{-23}$ J/K denotes the Boltzmann constant. The cut-off radius r_c beyond which the intermolecular interaction is neglected is 5.0σ.

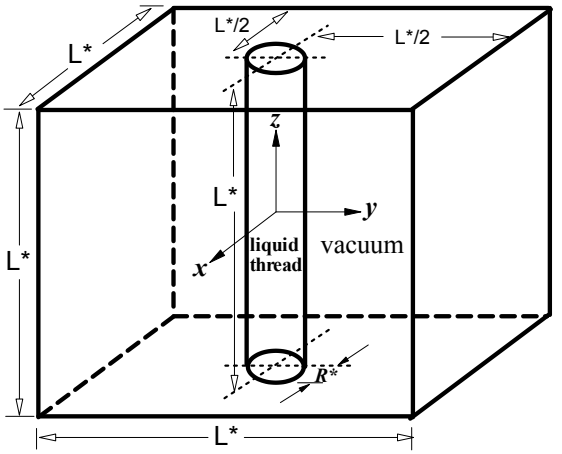

Figure 2: Illustration of the computational domain for the simulation of a liquid thread

The simulation domain is schematically shown in Fig.2, with periodic boundary conditions applied in all three directions. Simulation domain dimensions, temperatures and number of molecules, are listed in Table 1, together with some simulation results. The time integration of motion is performed by Gear's fifth predictor-corrector method [Haile (1992)] with a time step of t^*=0.001(i.e. 2.5 fs). Note that all quantities with an asterisk in this paper, such as L^*, R^*, ρ^*, t^*, etc., are non-dimensionalized in terms of σ, ε, and m, i.e. L^*=L/σ, $R^* = R/\sigma$, ρ^*=$N\sigma^3$/V, $t^* = t$ $(\varepsilon/m)^{1/2}/\sigma$, $T^* = k_BT/\varepsilon$.

In this research, a cylindrical liquid thread of length L^* and radius R^* is placed at the center of the computational domain and the remaining space is vacuum. The initial density of the liquid argon is ρ_L^*=0.819. The system temperature is kept at T^*=0.75 or 1.0. These dimensionless values correspond to ρ_L=1223 kg/m^3 for

Table 1: Simulation domain dimensions, temperatures, number of molecules, and simulation results

Case No.	L^*	R^*	T^*	N_{mol}	$\overline{f_\rho}$	Np
1	10	2	0.75	109	0.286	1
2	20	2	0.75	210	0.289	1
3	30	2	0.75	303	0.356	1
4	60	2	0.75	638	0.542	1
5	120	2	0.75	1221	0.635	2
6	240	2	0.75	2476	0.688	5
7	480	2	0.75	4929	0.690	10
8	10	3	0.75	235	0.341	intact
9	16	3	0.75	370	0.492	1
10	20	3	0.75	468	0.496	1
11	30	3	0.75	690	0.503	1
12	60	3	0.75	1395	0.616	1
13	120	3	0.75	2787	0.752	1
14	240	3	0.75	5590	0.805	2
15	480	3	0.75	11090	0.820	5
16	10	4	0.75	410	0.206	intact
17	20	4	0.75	824	0.555	intact
18	24	4	0.75	990	0.598	1
19	30	4	0.75	1225	0.611	1
20	60	4	0.75	2467	0.652	1
21	120	4	0.75	4943	0.741	1
22	240	4	0.75	9867	0.839	1
23	480	4	0.75	19709	0.857	3
24	10	4	1.0	407	0.001	intact
25	20	4	1.0	825	0.165	1
26	30	4	1.0	1235	0.195	1
27	60	4	1.0	2470	0.411	1
28	120	4	1.0	4927	0.487	1
29	240	4	1.0	9888	0.698	2
30	480	4	1.0	19797	0.736	4

argon and T=70K or 93.3K. Note that these two temperatures are below the critical temperature(150K)of argon.

The procedure for MD simulation includes three stages : initialization, equilibration and production. Initially, equilibration is performed for liquid argon molecules

in a rectangular parallelepiped with length and width equal to the liquid thread diameter (D^*=2R^*=4, 6, 8) and with height equal to the side length of the computational domain (L^*=10, 16, 20, 24, 30, 60, 120, 240, 480). The initial velocities of molecules are decided by normal random numbers. Velocity rescaling is performed at each time step by Eq.(2) to make sure that the molecules are at the desired temperature T^* :

$$v_i^{new} = v_i^{old}\sqrt{\frac{T_D}{T_A}} \tag{2}$$

where v_i^{new} and v_i^{old} are the velocities of molecule i after and before correction, respectively, and T_D and T_A are the desired and the actual molecular temperatures, respectively. The liquid molecules are equilibrated for 10^6 time steps at the desired temperature T^*. The achievement of equilibrium state is confirmed by obtaining the radial distribution function. After the liquid molecules are equilibrated, the rectangular parallelepiped for the liquid molecules is truncated to the desired cylindrical liquid thread by removing unwanted regions. The cylindrical liquid thread then is put into the computational domain and the production stage proceeds. A minimum image method and the Verlet neighbor list scheme [Haile (1992)] to keep track of which molecules are actually interacting at a given time interval of 0.005 are used in the equilibration and the production stages.

3 Results and Discussions

3.1 Liquid Thread Vaporization Process

In the following discussion, a cylindrical liquid thread of length L^* and radius R^* is placed at the center of the simulation domain and the remaining space is in vacuum, as illustrated in Fig.2. Simulation domain dimensions, temperatures and number of molecules, are listed in Table 1.

Figures 3∼5 show the vaporization processes of liquid threads at T^*=0.75(cases 1∼23 in Table 1). Note that L^*=120 and R^*=3 correspond to L=42.5nm and R=1.06nm, respectively. It is found that whenR^*=2, the liquid thread breaks up into drops for all fundamental cell lengths. For L^*=10, 20, 30 and 60, the liquid thread ruptures only from its two ends, i.e. the top and bottom surfaces of the fundamental cell, and gets shorter due to the contraction motion in its axial direction. Only one liquid particle is formed. On the other hand, for L^*=120, 240 and 480, the thread ruptures not only from the top and bottom surfaces of the fundamental cell but also from its interior section. The number of liquid particles produced for L^*=120, 240 and 480 is 2, 5 and 10, respectively. During the vaporization process, collision and coalescence of the liquid particles occur. The two liquid particles produced for L^*=120

coalesce into one liquid particle. The number of liquid particles at t*=1000 for L^*=240 and 480 is 3 and 5, respectively.

WhenR^*=3, the liquid thread breaks up into drops for all fundamental cell lengths except L^*=10 for which the liquid thread remains intact. For L^*=16, 20, 30, 60 and 120, the liquid thread ruptures merely from its two ends and only one liquid particle is formed. For L^*=240 and 480, the thread ruptures not only from the top and bottom surfaces of the fundamental cell but also from its interior section. The number of liquid particles produced for L^*=240 and 480 is 2 and 5, respectively. During the vaporization process, collision and coalescence of the liquid particles occur. The liquid particles for L^*=240 and 480 both coalesce into one liquid particle.

WhenR^*=4, the liquid thread remains intact for L^*=10 and 20. For L^*=24, 30, 60, 120 and 240, the liquid thread ruptures merely from its two ends and only one liquid particle is formed. For L^*=480, the thread ruptures not only from the top and bottom surfaces of the fundamental cell but also from its interior section. Three liquid particles are produced. The liquid particles eventually coalesce into one liquid particle.

Figure 6 shows the vaporization processes for liquid threads of R^*=4 at T^*=1.0(cases 24$\sim$30 in Table 1). Unlike the liquid threads of the same radius R^*=4 at a lower temperature T^*=0.75(cases 16$\sim$23 in Table 1), the liquid thread remains intact only for L^*=10. For L^*=20, 30, 60 and 120, the liquid thread ruptures from its two ends, i.e. the top and bottom surfaces of the fundamental cell, and only one liquid particle is formed. For L^*=240 and 480, the thread ruptures not only from the top and bottom surfaces of the fundamental cell but also from its interior section. The number of liquid particles produced for L^*=240 and 480 is 2 and 4, respectively. During the vaporization process, collision and coalescence of the liquid particles occur. The liquid particles eventually coalesce into one liquid particle.

From the above discussion for Figs.3$\sim$6, the following observations can be obtained.

First, if the fundamental cell length is long enough, more than one liquid particle may be produced in the cell. Under such situation, the liquid thread ruptures not only from its two ends but also from the interior of the fundamental cell. On the other hand, if the fundamental cell length is small, the liquid thread may remain intact or produce only one liquid particle in the cell. If the thread breaks up, it ruptures from its two ends only, i.e. the top and bottom surfaces of the fundamental cell, but not from its interior.

Second, a liquid thread with a longer fundamental cell length may produce more liquid particles in the cell.

Third, a thinner liquid thread may produce more liquid particles in the cell.

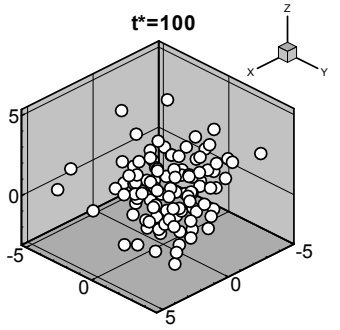

R*=2, L*=10, T*=0.75

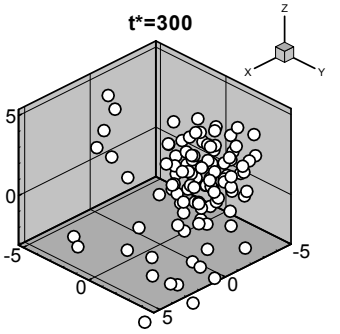

R*=2, L*=10, T*=0.75

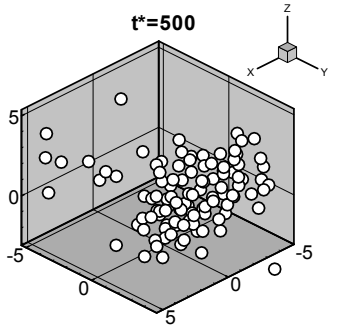

R*=2, L*=10, T*=0.75

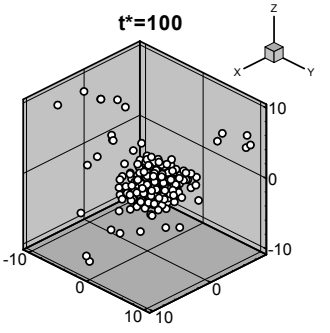

R*=2, L*=20, T*=0.75

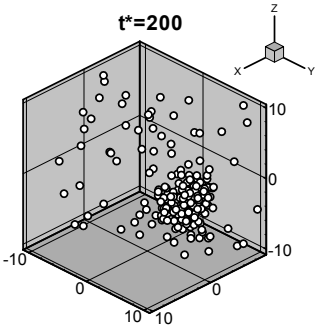

R*=2, L*=20, T*=0.75

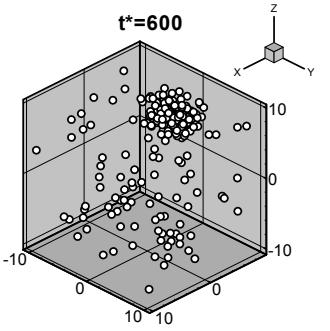

R*=2, L*=20, T*=0.75

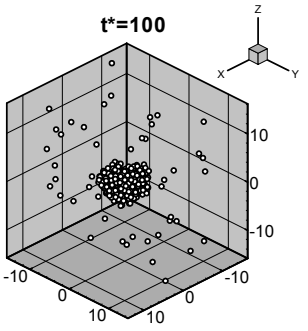

R*=2, L*=30, T*=0.75

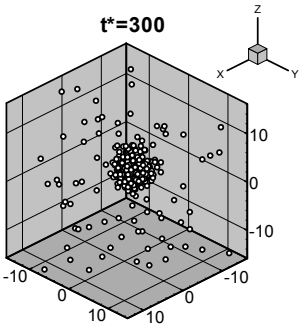

R*=2, L*=30, T*=0.75

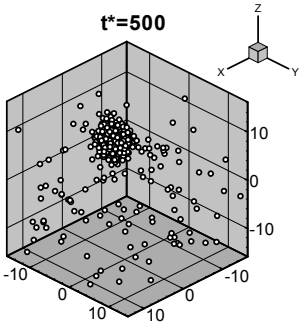

R*=2, L*=30, T*=0.75

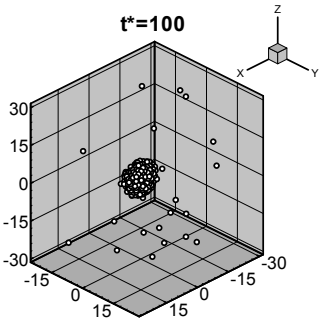

R*=2, L*=60, T*=0.75

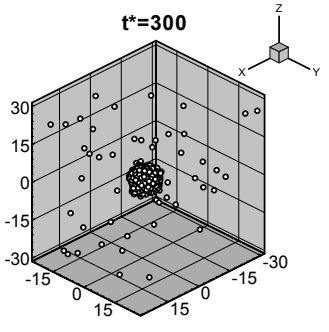

R*=2, L*=60, T*=0.75

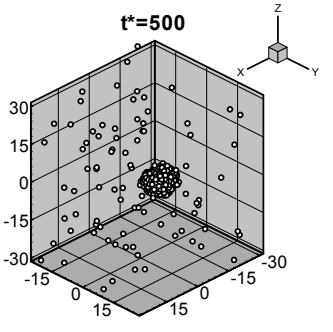

R*=2, L*=60, T*=0.75

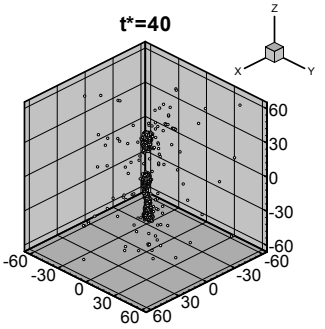

R*=2, L*=120, T*=0.75

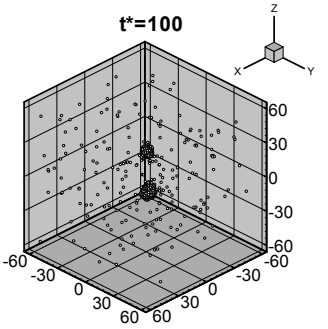

R*=2, L*=120, T*=0.75

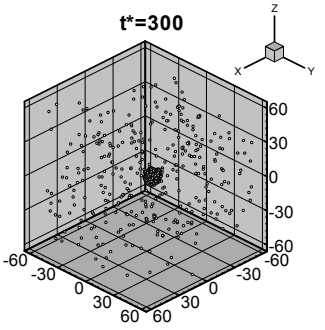

R*=2, L*=120, T*=0.75

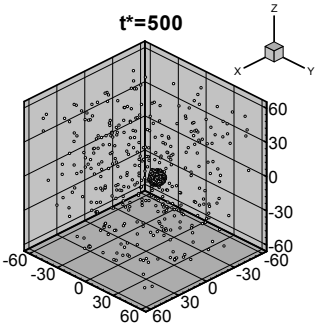

R*=2, L*=120, T*=0.75

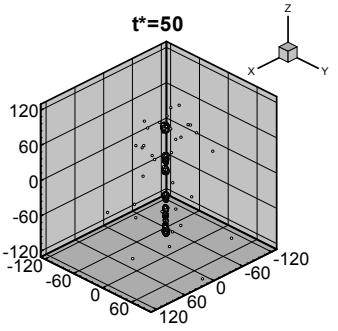

R*=2, L*=240, T*=0.75

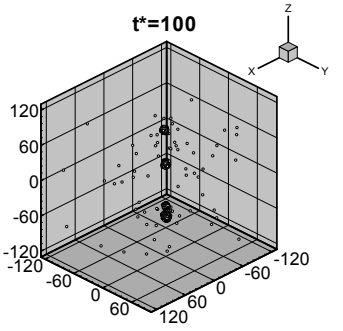

R*=2, L*=240, T*=0.75

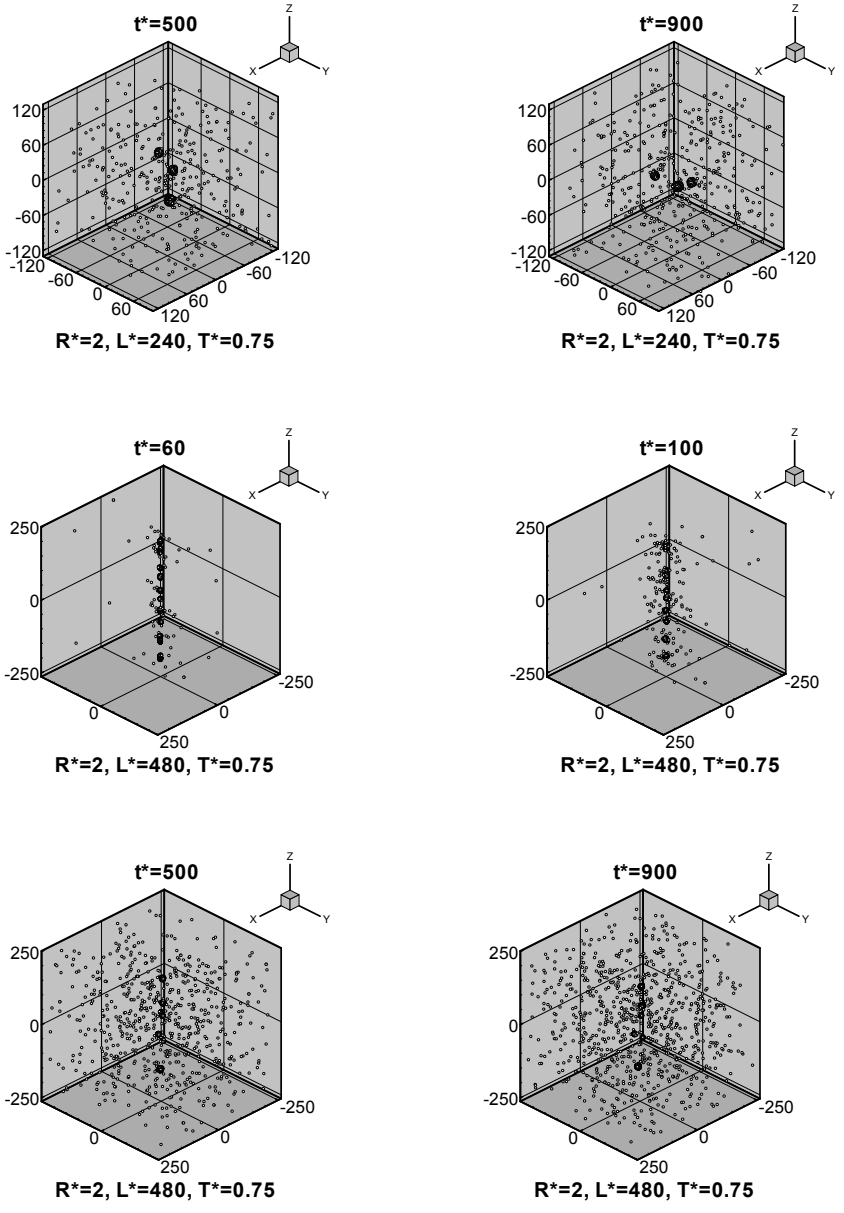

Figure 3: Vaporization processes of liquid threads of R^*=2 at T^*=0.75

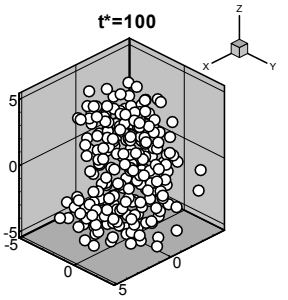

R*=3, L*=10, T*=0.75

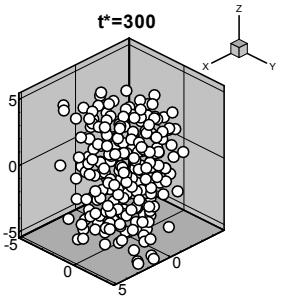

R*=3, L*=10, T*=0.75

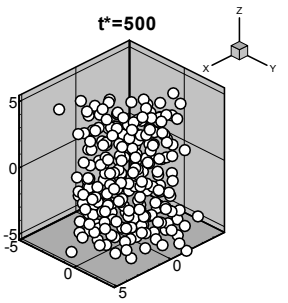

R*=3, L*=10, T*=0.75

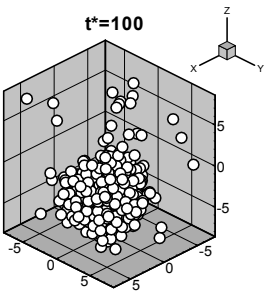

R*=3, L*=16, T*=0.75

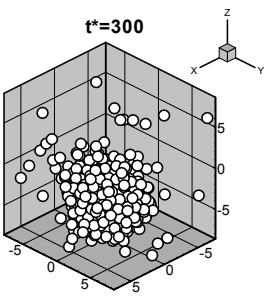

R*=3, L*=16, T*=0.75

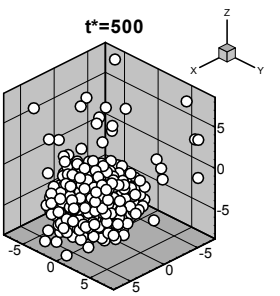

R*=3, L*=16, T*=0.75

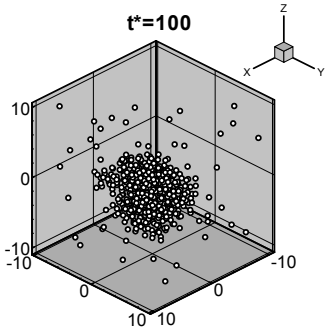

R*=3, L*=20, T*=0.75

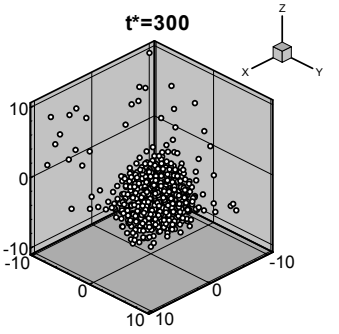

R*=3, L*=20, T*=0.75

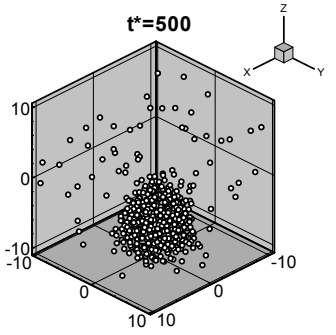

R*=3, L*=20, T*=0.75

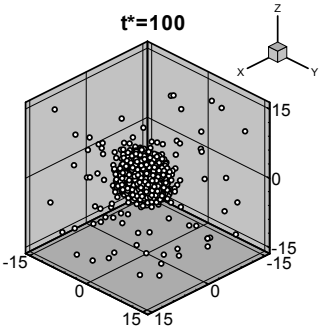

R*=3, L*=30, T*=0.75

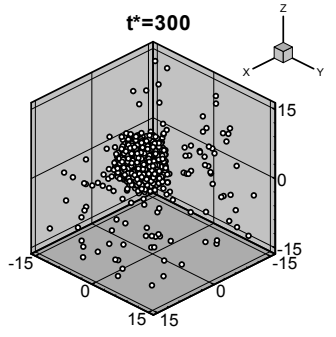

R*=3, L*=30, T*=0.75

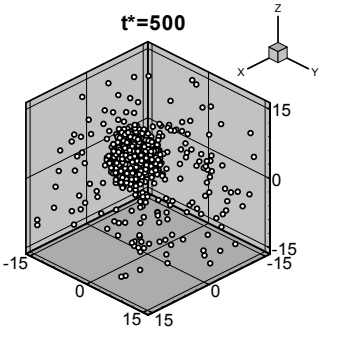

R*=3, L*=30, T*=0.75

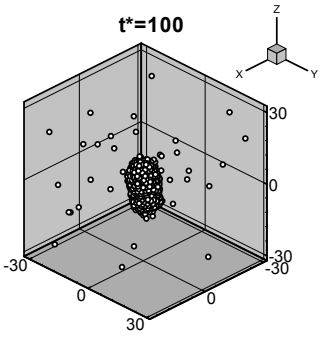

R*=3, L*=60, T*=0.75

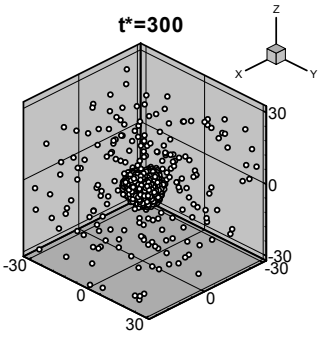

R*=3, L*=60, T*=0.75

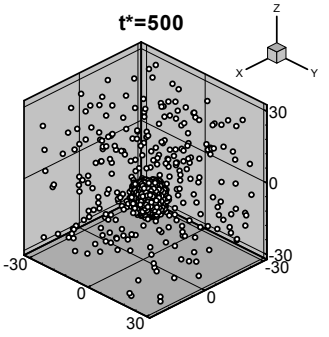

R*=3, L*=60, T*=0.75

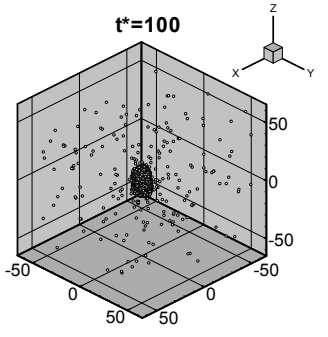

R*=3, L*=120, T*=0.75

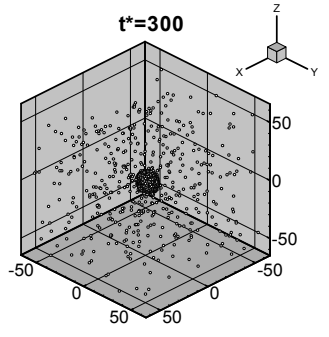

R*=3, L*=120, T*=0.75

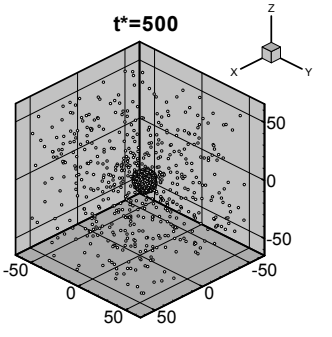

R*=3, L*=120, T*=0.75

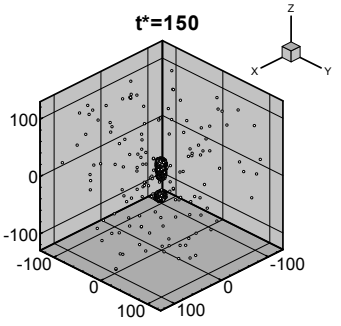

R*=3, L*=240, T*=0.75

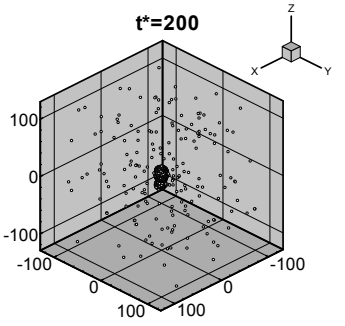

R*=3, L*=240, T*=0.75

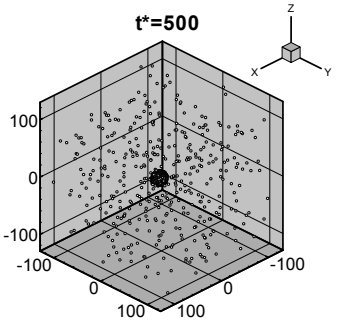

R*=3, L*=240, T*=0.75

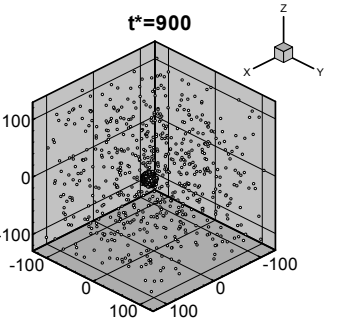

R*=3, L*=240, T*=0.75

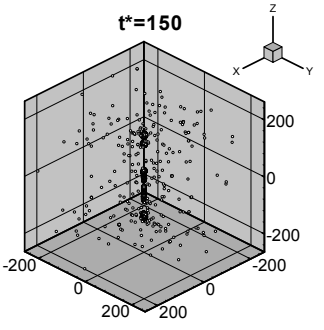

R*=3, L*=480, T*=0.75

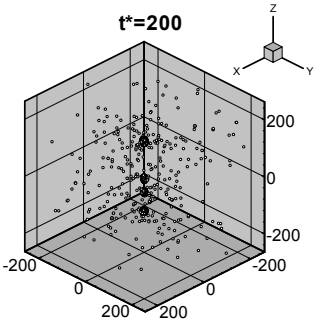

R*=3, L*=480, T*=0.75

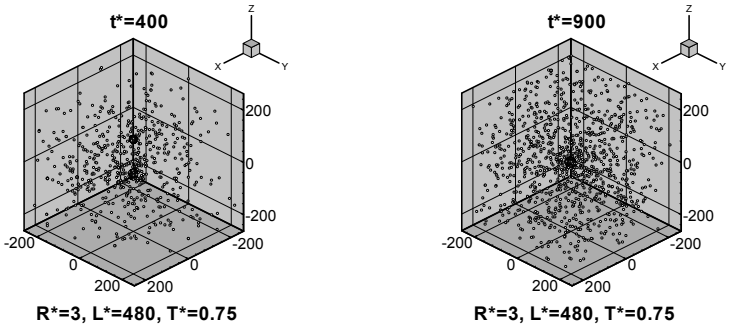

Figure 4: Vaporization processes of liquid threads of R^*=3 at T^*=0.75

Fourth, a liquid thread at a higher temperature may produce more liquid particles.

3.2 Stability Analysis

According to the classical theory by Rayleigh (1879), the radius of the liquid thread, R, is related to the critical wavelength of perturbation, λ_c , as

$$\lambda_c = 2\pi R \tag{3}$$

A liquid thread will break up into drops if the axial wavelength of the surface perturbation $L>\lambda_c$. If $L<\lambda_c$, the thread is stable and will remain intact. Owing to the periodic boundary conditions in this study, the fundamental cell size L^* can be regarded as the longest wavelength of the perturbation.

For R^*=2, λ_c^* is 12.6. According to Rayleigh's stability criterion, a liquid thread of radius R^*=2 and length L^*=10 is expected to be stable and remain intact. However, from Fig.3 or Table 1(Case 1), it is seen that the liquid thread of R^*=2 and L^*=10 is unstable, which implies that Rayleigh's stability criterion overpredicts the stable domain as compared to the MD simulation results. Rayleigh's stability criterion holds for the remaining liquid threads with$L^*>\lambda_c^*$(L^*=20$\sim$480), which are unstable and break up into drop(s).

For R^*=3, λ_c^* is 18.9. From Fig.4 or Table 1(Cases 8 and 9), the liquid thread of R^*=3 and L^*=10 remains intact while the liquid thread of R^*=3 and L^*=16 is unstable. Rayleigh's stability criterion holds for the former case but violates the MD simulation results for the latter case. The remaining liquid threads with$L^*>\lambda_c^*$(L^*=20$\sim$480)are unstable and break up into drop(s). Rayleigh's stability criterion holds for these cases.

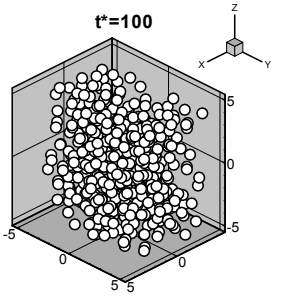

R*=4, L*=10, T*=0.75

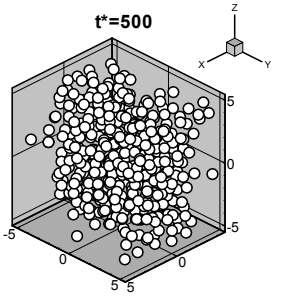

R*=4, L*=10, T*=0.75

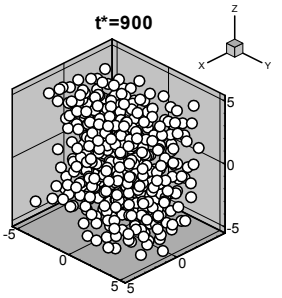

R*=4, L*=10, T*=0.75

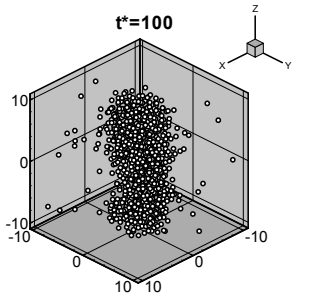

R*=4, L*=20, T*=0.75

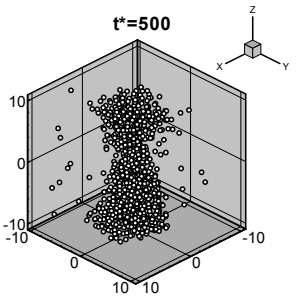

R*=4, L*=20, T*=0.75

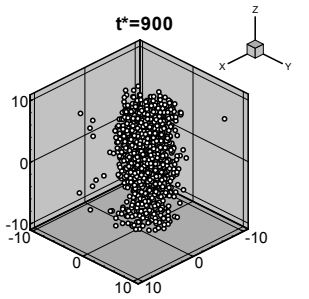

R*=4, L*=20, T*=0.75

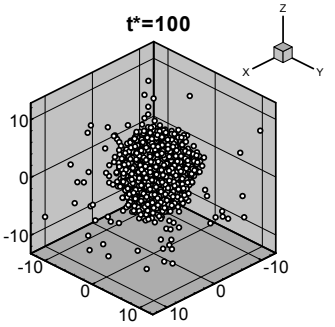

R*=4, L*=24, T*=0.75

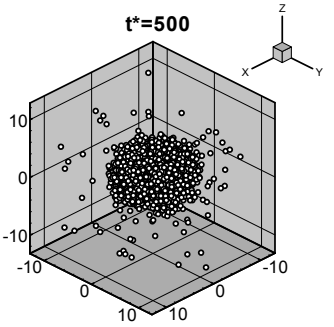

R*=4, L*=24, T*=0.75

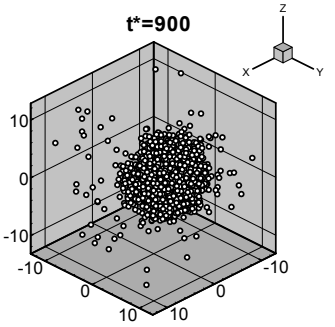

R*=4, L*=24, T*=0.75

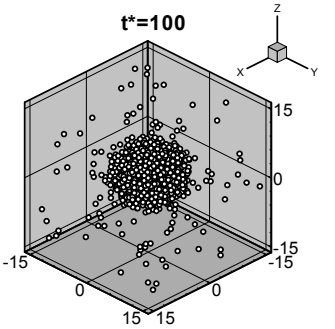

R*=4, L*=30, T*=0.75

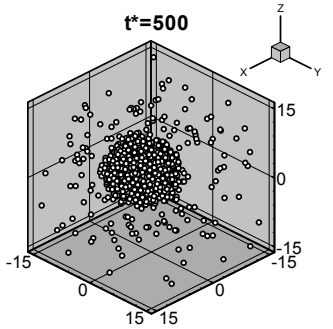

R*=4, L*=30, T*=0.75

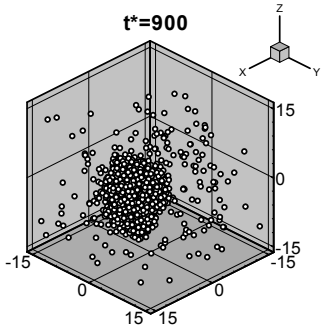

R*=4, L*=30, T*=0.75

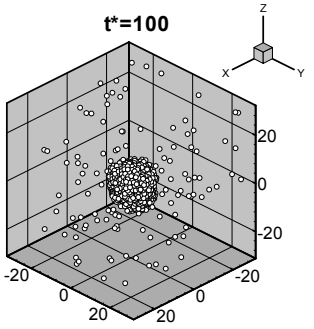

R*=4, L*=60, T*=0.75

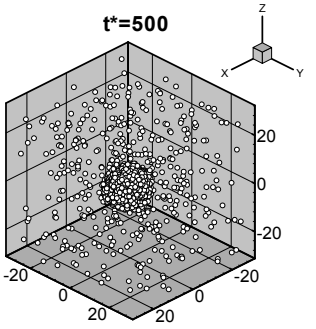

R*=4, L*=60, T*=0.75

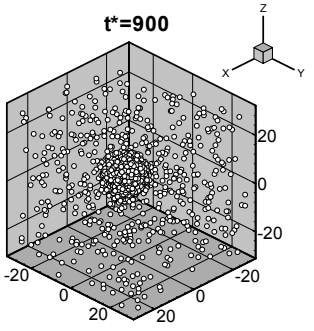

R*=4, L*=60, T*=0.75

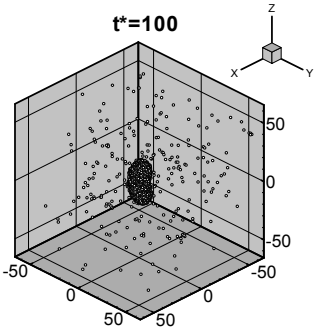

R*=4, L*=120, T*=0.75

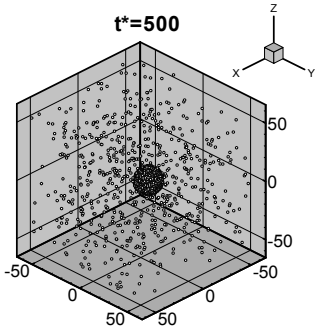

R*=4, L*=120, T*=0.75

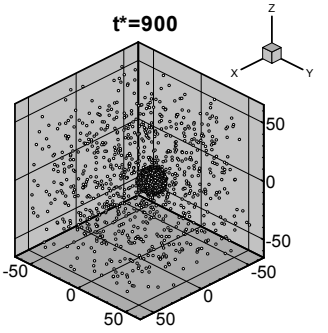

R*=4, L*=120, T*=0.75

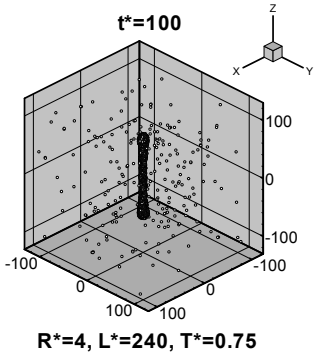

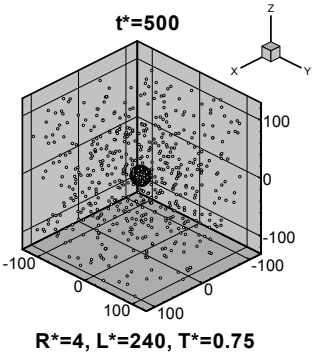

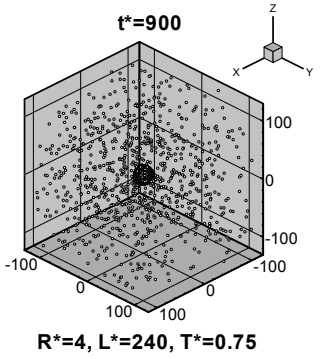

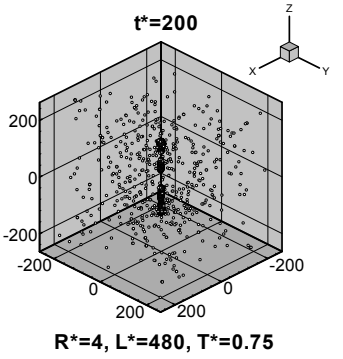

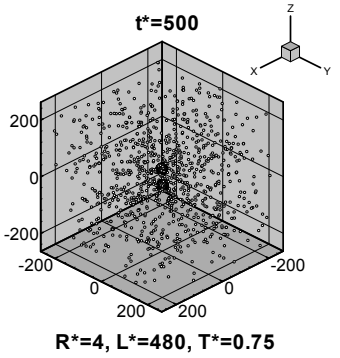

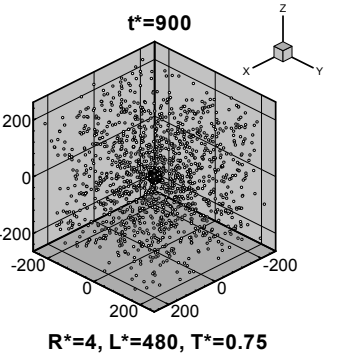

Figure 5: Vaporization processes of liquid threads of R^*=4 at T^*=0.75

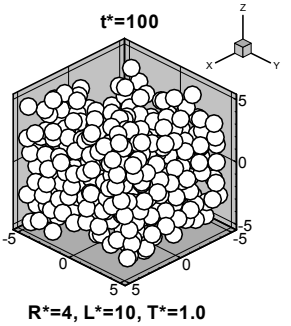

R*=4, L*=10, T*=1.0

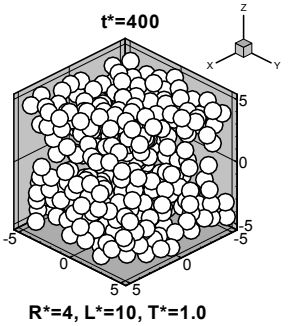

R*=4, L*=10, T*=1.0

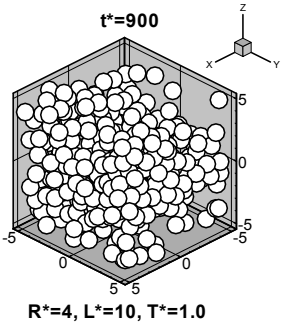

R*=4, L*=10, T*=1.0

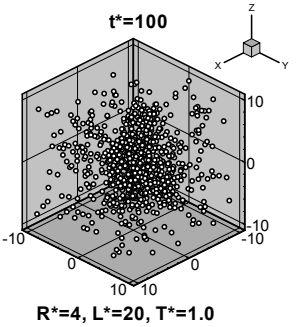

R*=4, L*=20, T*=1.0

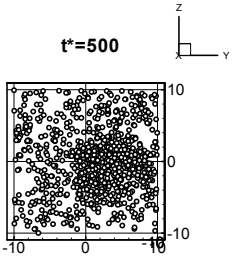

R*=4, L*=20, T*=1.0

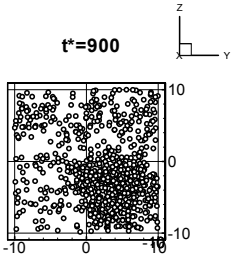

R*=4, L*=20, T*=1.0

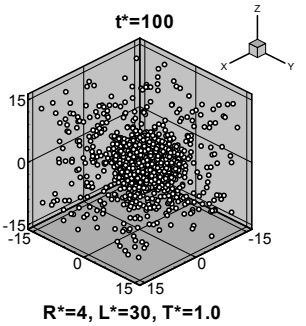

R*=4, L*=30, T*=1.0

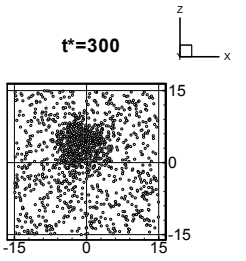

R*=4, L*=30, T*=1.0

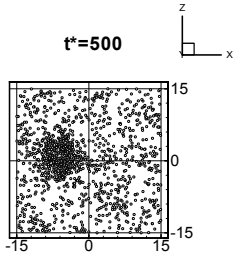

R*=4, L*=30, T*=1.0

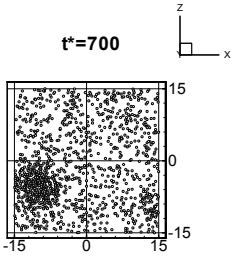

R*=4, L*=30, T*=1.0

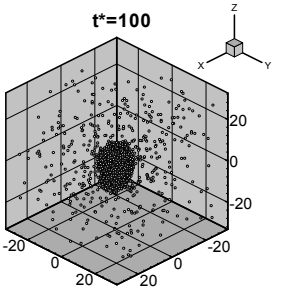

R*=4, L*=60, T*=1.0

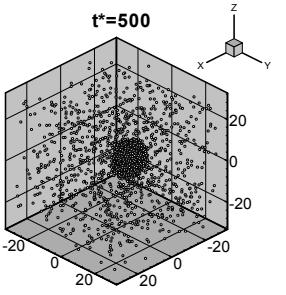

R*=4, L*=60, T*=1.0

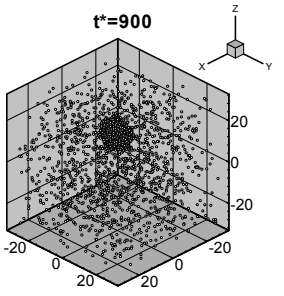

R*=4, L*=60, T*=1.0

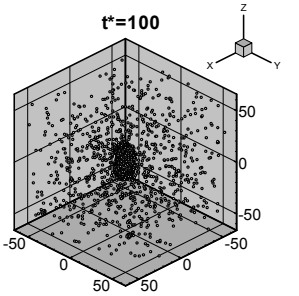

R*=4, L*=120, T*=1.0

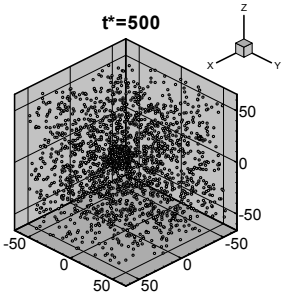

R*=4, L*=120, T*=1.0

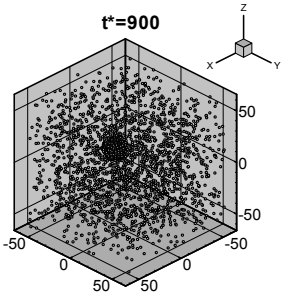

R*=4, L*=120, T*=1.0

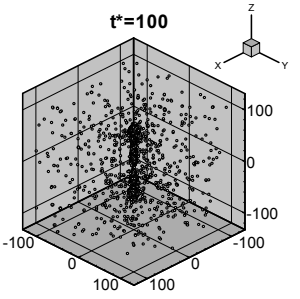

R*=4, L*=240, T*=1.0

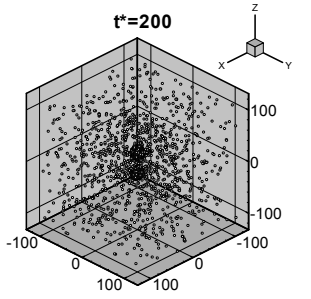

R*=4, L*=240, T*=1.0

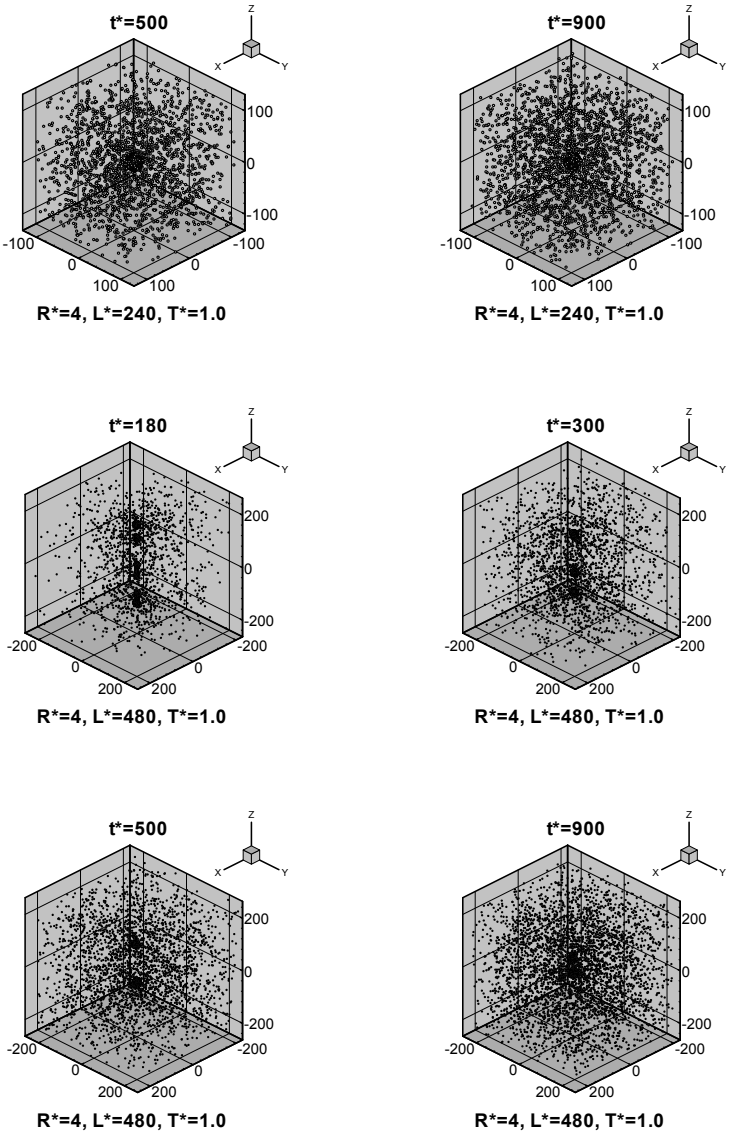

Figure 6: Vaporization processes of liquid threads of R^*=4 at T^*=1.0

For R^*=4, λ_c^* is 25.2. From Fig.5 or Table 1(Cases 16∼23), the liquid threads of L^*=10 and 20 remain intact while the liquid thread of L^*=24 is unstable. Rayleigh's stability criterion holds for the first two cases but violates the MD simulation results for the third case. The remaining liquid threads with$L^*>\lambda_c^*$(L^*=30∼480)are unstable and break up into drop(s). Rayleigh's stability criterion holds for these cases.

If the temperature of the liquid threads of R^*=4 is increased to T^*=1.0, from Fig.6 or Table 1(Cases 24∼30), only the liquid thread of L^*=10 remains intact while, in contrast to the situation of T^*=0.75, the liquid thread of L^*=20 is unstable. Rayleigh's stability criterion holds for the former case but violates the MD simulation results for the latter case. The remaining liquid threads with$L^*>\lambda_c^*$(L^*=30∼480)are unstable and break up into drop(s). Rayleigh's stability criterion holds for these cases.

Recently, Kim, Lee, Han and Park (2006) proposed a new linear relation from their MD simulation results. From their study, Rayleigh's linear relation can be modified as

$$\lambda_c = 2.44\pi(R - 1.23) \tag{4}$$

From Eq.(4), λ_c^* for R^* of 2, 3 and 4 are 5.9, 13.6 and 21.2, respectively. Then, from Table 1(Cases 1∼23), it is seen that Kim's stability criterion holds for the liquid threads at T^*=0.75. On the other hand, at T^*=1.0(Cases 24∼30), the liquid thread of R^*=4 and L^*=10 remains intact while the liquid thread of R^*=4 and L^*=20 is unstable. Kim's stability criterion holds for the former case but violates the MD simulation results for the latter case. The remaining liquid threads with$L^*>\lambda_c^*$(L^*=30∼480)are unstable and break up into drop(s). Kim's stability criterion holds for these cases.

From the above discussion, the following observations can be made.

First, a liquid thread with a longer fundamental cell length is more unstable.

Second, a thinner liquid thread is more unstable.

Third, a liquid thread at a higher temperature is more unstable.

Fourth, the trends of linear stability theories agree with MD simulation results. However, Rayleigh's stability criterion overpredicts stable domain as compared to the MD simulation results. Kim's stability criterion gives more accurate predictions. However, it overpredicts the stable domain at a higher temperature as compared to the MD simulation results.

3.3 Density Distribution

In practical applications, e.g. combustor or printer, faster vaporization is usually desirable. Criteria have to be made to quantify the discussion regarding the vapor-

ization process of a liquid thread. In this research, a liquid thread is considered to vaporize faster if the distribution of molecules reaches uniform state quicker during the vaporization process. This criterion essentially concerns with the evolution of the density distribution. The density at a specified point in the fundamental cell can be defined as

$$\rho = \lim_{\delta V \to 0} \frac{\delta N}{\delta V} \tag{5}$$

where δV is a small volume surrounding the point considered and δN is the number of molecules inside the volume δV. The density defined by Eq.(5) is actually an averaged density of a small volume surrounding the point considered. The value will approach the density of a specified point if the volume δV shrinks to that point. However, for a meaningful density field, the volume δV can not be too small because when δV becomes too small, it is difficult to obtain a definite value for $\delta N/\delta V$. In this study, the volume δV is taken to be a sphere with non-dimensionalized radius R^*=2 and with its center located at the point considered. This is an optimal choice after numerical test.

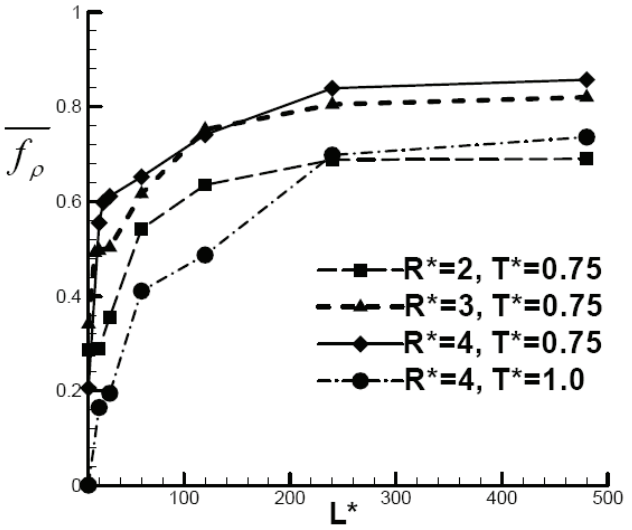

Figure 7: Comparison of time averaged density uniformity factor, $\overline{f_\rho}$, for liquid threads of different radius, length and temperature

The time averaged density uniformity factor,$\overline{f_\rho}$, in a time interval of $t*$=0 to 1000, as shown in Fig.7 or listed in Table 1, can be used to indicate the vaporization speed

of a liquid thread. The density uniformity factor, f_ρ , is defined as

$$f_\rho = \frac{\sum_N \left(\rho^* - \rho^*_{eq}\right)_{t*} \Delta V}{\sum_N \left(\rho^* - \rho^*_{eq}\right)_{t*=0} \Delta V} \tag{6}$$

where N is the total number of molecules in the fundamental cell, i.e. N_{mol} in Table 1, ρ^* and V are the density and volume of molecule i, respectively, as defined by Eq.(5), and ρ^*_{eq} is the density value when the molecules are uniformly distributed, i.e. $\rho^*_{eq} \equiv N_{mol}/$ Vol, where Vol is the volume of the fundamental cell. The density uniformity factor, f_ρ , as defined by Eq.(6) represents the deviation from uniform state. From Fig.7 or Table 1, the following observations can be drawn.

First, a liquid thread with a shorter fundamental cell length evaporates quicker. Take the liquid threads of R^*=2(Cases 1$\sim$7)as an example. The liquid thread of L^*=10(Case 1)produces one liquid particle while the liquid thread of L^*=480(Case 7)produces ten liquid particles. The length of the latter liquid thread is forty-eight times of the former one. This implies that if forty-eight liquid threads of L^*=10 are connected in series, there will be forty-eight liquid particles. It is known that molecular interaction plays an important role in the vaporization process. More liquid particles can provide more molecular interactions and this is conducive to vaporization.

Second, a liquid thread evaporates quicker at a higher temperature.

Third, a liquid thread with a higher $\overline{f_\rho}$ is more unstable and produces more liquid particles in the fundamental cell.

4 Conclusions

In this study, the instability of a liquid thread is investigated by MD simulation. It is found that a liquid thread is more unstable and produces more liquid particles in the fundamental cell when it is thinner or at a higher temperature. In addition, a liquid thread with a longer fundamental cell length is also more unstable and produces more liquid particles in the fundamental cell, but it evaporates slower. The trends of linear stability theories agree with MD simulation results. However, Rayleigh's stability criterion overpredicts stable domain as compared to the MD simulation results. Kim's stability criterion gives more accurate predictions but overpredicts the stable domain at a higher temperature. Finally, a liquid thread with a higher time averaged density uniformity factor,$\overline{f_\rho}$, is more unstable and produces more liquid particles in the fundamental cell.

Acknowledgement: The author gratefully acknowledges the grant support from

the National Science Council, Taiwan, R.O.C., under the contract NSC98-2221-E-150-041.

References

Chen, W. H.; Cheng, H. C.; Hsu, Y. C. (2007) : Mechanical properties of carbon nanotubes using molecular dynamics simulations with the inlayer van der Waals interactions. *CMES: Computer Modeling in Engineering & Sciences*, vol.20, no.2, pp.123-145.

Goren, S. (1962) : The instability of an annular thread of fluid. *Journal of Fluid Mechanics*, vol.12, pp.309-319.

Haile, J. M.(1992): Molecular Dynamics Simulation. John Wiley & Sons, New York, chap.5.

Kawano, S. (1998) : Molecular dynamics of rupture phenomena in a liquid thread. *Physical Review*, E, vol.58, no.4, pp.4468-4472.

Kim, B. G.; Lee, J. S.; Han, M.; Park, S. (2006) : A molecular dynamics study on stability and thermophysical properties of nano-scale liquid threads. *Nano-scale and Micro-scale Thermophysical Engineering*, vol.10, pp.283-304.

Koplik, J.; Banavar, J. R. (1993) : Molecular dynamics of interface rupture. *Physics of Fluids*, A, vol.5, no.3, pp.521-536.

Liu, D. S.; Tsai, C.Y. (2009): Estimation of thermo-elasto-plastic properties of thin-film mechanical properties using MD nanoindentation simulations and an inverse FEM/ANN computational scheme. *CMES: Computer Modeling in Engineering & Sciences*, vol.39, no.1, pp.29-48.

Lord Rayleigh(1879): On the stability of jets. *Proceedings of the London Mathematical Society*, vol.10, pp.4-13.

Matsumoto, R.; Nakagaki, M.; Nakatani, A.; Kitagawa, H. (2005) : Molecular-dynamics study on crack growth behavior relevant to crystal nucleation in amorphous metal. *CMES: Computer Modeling in Engineering & Sciences*, vol.9, no.1, pp.75-84.

Min, D.; Wong, H. (2006) : Rayleigh's instability of Lennard-Jones liquid nanothreads simulated by molecular dynamics. *Physics of Fluids*, vol.18, 024103.

Nair, A. K.; Farkas, D.; Kriz, R. D. (2008) : Molecular dynamics study of size effects and deformation of thin films due to nanoindentation. *CMES: Computer Modeling in Engineering & Sciences*, vol.24, no.3, pp.239-248.

Namilae, S.; Chandra, U.; Srinivasan, A; Chandra, N.(2007): Effect of interface modification on the mechanical behavior of carbon nanotube reinforced composites using parallel molecular dynamics simulations. *CMES: Computer Modeling in*

Engineering & Sciences, vol.22, no.3, pp.189-202.

Tang, W.; Advani, S. G. (2008) : Dynamic simulation of carbon nanotubes in simple shear flow. *CMES: Computer Modeling in Engineering & Sciences*, vol.25, no.3, pp.149-164.

Tang, W.; Advani, S. G. (2007) : Non-equilibrium molecular dynamics simulation of water flow around a carbon nanotube. *CMES: Computer Modeling in Engineering & Sciences*, vol.22, no.1, pp.31-40.

Tomotika, S. (1935) : On the instability of a cylindrical thread of a viscous liquid surrounded by another viscous liquid. *Proceedings of the Royal Society of London,* Series A, Mathematical and Physical Sciences, vol.150, no.870, pp.322-337.

Weber, C. (1931) : Zum zerfall eines ussigkeitsstrahles. *Zeitschrift fur Angewandte Mathematik und Mechanik*. vol.11, no.2, pp.136-154.

Wei, C.; Srivastava, D.; Cho, K.(2002): Molecular dynamics study of temperature dependent plastic collapse of carbon nanotubes under axial compression. *CMES: Computer Modeling in Engineering & Sciences*, vol.3, no.2, pp.255-261.

Yeh, C. L. (2005) : Turbulent flow investigation inside and outside plain-orifice atomizers with rounded orifice inlets. *Heat and Mass Transfer*, vol.41, no.9, pp.810-823.

Yeh, C. L. (2009) : Molecular dynamics simulation for the atomization process of a nanojet. *CMES: Computer Modeling in Engineering & Sciences*, vol.39, no.2, pp.179-200.